



Received: 01 June, 2023

Accepted: 13 June, 2023

Published: 14 June, 2023

*Corresponding authors: Jin Peng, Department of Chemistry, Linyi University, China, Tel: 19560832762; Email: linqingya1007@163.com

Keywords: TX; Structural characteristics; Hydration number; Air-water interface; MD simulations

Copyright License: © 2023 Peng J. This is an open-access article distributed under the terms of the Creative Commons Attribution License, which permits unrestricted use, distribution, and reproduction in any medium, provided the original author and source are credited.

<https://www.peertechzpublications.com>



Review Article

Molecular dynamics of Triton X surfactant molecules with different PEO chain lengths at the air/water interface

Jin Peng*

Department of Chemistry, Linyi University, China

Abstract

This paper focuses on the structural properties and interface behavior of TX-5, TX-114, and TX-100 molecules at the air/water interface. The results of the density profile show that the polar O atoms of the three TX molecules are basically located on the water surface, and the whole TX molecule is almost parallel to the water surface. The results of the order parameters show that the order parameters of the three TX molecules on the interface are similar and relatively ordered. The TX-100 molecule has the largest gauche defect value. The hydration number of TX molecules at the interface was similar to that of TX molecules in micelles, and the hydration number of PEO chains showed obvious zigzag changes. The research of this paper provides a reference for the further development of TX series micellar and surfactant molecules in the field of pharmaceutical and daily use.

Introduction

Surfactant is first adsorbed to the interface before forming micelles in an aqueous solution and has a variety of surface active properties, including foaming properties, fiber cleaning properties, water hardness, etc. [1]. Adsorbable properties on solid-liquid surfaces are important for many industrial and technical processes (such as processing washing products, water treatment, enhanced oil recovery, etc.) [2], and are also widely used at the gas-water interface, such as food production, foam fractionation, and fermentation processes [3]. Quite a few technicians [3-7] use the adsorption properties of surfactants at the air/water interface to reduce surface tension, control foaming, foam stability, etc. Foam behavior is fundamentally dependent on the properties of the surfactant added [8] and especially its structure [9,10]. Different types of surfactants have different molecular structures, and most of the hydrophilic groups in the structure of non-ionic surfactants are Polyethylene Oxide (PEO) chains [11]. In the same series of non-ionic surfactants, different chain lengths will affect their adsorption properties [8]. The Triton X series is a major class of non-ionic surfactants, TX-114 is one of the most commercially

and industrially used cleaners and emulsifiers [1] and TX-100 is also of industrial importance in the preparation of foams [12], so it has been widely studied and used.

Relevant experimental studies have shown that the adsorption effect of surfactants is an important factor in determining important properties such as foaming, wetting, emulsification, solubilization, drug delivery, and biological activity [1]. Fainerman, et al. [13] studied the adsorption kinetics of TX-100 at the water-air interface using the maximum bubble pressure method, the inclined plate method, and the oscillating jet method and showed that all PEO chains can be located in the surface layer when the adsorption capacity or surface pressure of TX-100 is very small. The dynamic behavior of many systems (such as foam stability, etc.) is controlled by the adsorption of surfactant at the air/water interface [14]. For example, Agneta, et al. [15] found in the experiment that foam stability is generated by the presence of TX-100 surfactant at the air/water interface. Computer simulation is an important tool for studying interface systems, which can obtain more information about the dynamics and structural properties of interface problems at the molecular

level, which is not easy to obtain from experimental technical means [16]. As early as 1994, Tarek, et al. [17] conducted MD simulations of the structure and behavior of tetracyl-trimethyl ammonium bromide (C₁₄TAB) at the air/water interface. They analyzed the structure of hydrocarbon chains and found that the chains were highly disordered and their internal structure depended on vertical position relative to the interface. Later, Xu, et al. [18] also used the MD simulation method to study the influence of Polyvinyl Alcohol (PVA) molecules on the structure of sodium dodecyl ether sulfate containing a polyethylene oxide group (SLE1S) adsorbed on the air/water interface. The results showed that increasing the surface density of SLE1S would increase the interface thickness. And forces SLE1S and PVA molecules to migrate to varying degrees into the air (actually the vacuum). In addition, Chanda, et al. [19] studied the adsorption properties of monomolecular dodecyl hexaethylene glycol (C₁₂E6) at the air/water interface by using MD simulation at constant volume and temperature. The study showed that due to the strong interaction between surfactants and water, its long polar head group preferred the water layer. Other researchers have explored the related properties of TX-100, another very important nonionic surfactant, at the air/water interface. For example, Parra, et al. [12] studied the effect of TX-100 on the interfacial activity of ionic surfactants SDS, CTAB and SDBS at the air/water interface by using MD simulation method and found that the presence of TX-100 at the air/water interface would reduce the interface thickness of water layer.

In order to make full use of the interfacial activity of the TX family of surfactants, the structural characteristics of TX-5, TX-114 and TX-100 molecules with different PEO chain lengths at the air/water interface and their interactions with water were investigated by molecular dynamics simulation. The differences and connections between the three systems were compared in various aspects.

Simulation detail

Materials and methods

The chemical structures and basic information of Triton-X are from the ATB force field.

Firstly, Gaussian 09 software [20] was used to optimize the geometric structure of TX-5, TX-114, and TX-100 molecules, and the basic group was B3LYP/6-31g(d). The structure is then submitted to ATB [21,22] to generate bond and non-bond resultant field parameters. This parameter is compatible with the Gromos 54A7 force field parameter. Water molecules use an SPC model.

The simulation uses a 10×10×30 nm³ rectangular box with the Z axis perpendicular to the interface. In preparation for the initial configuration of the simulation, a water box (10×10×10 nm³) was placed in the center of the box and filled with water molecules. Then, two identical TX molecules are placed on both sides of the water box to form the water-air interface. The size of the upper and lower air boxes on both sides is 10×10×10 nm³, and the TX molecules are perpendicular to the water surface,

which is the same for all three systems. The reason for placing the same TX molecule in each of the upper and lower interfaces is to facilitate comparison.

All simulations were calculated using the Gromacs 2021 software package [23]. The steepest descent method is used to minimize the energy of the initial configuration. Then, the MD trajectory was obtained after 200 ns NVT simulation at 298 K temperature. In this paper, the trajectory of the last 30 ns is used to analyze the results.

Hydrogen bonding was restricted by the LINCS algorithm [24]. Meanwhile, periodic boundary conditions were used in all directions, and a time step of 2 fs was used for all simulated environment variables. The simulated environment is closest to the experimental conditions. VMD [25] program was used to realize all visualization of MD locus.

For comparison, the TX molecules on the upper and lower interfaces are placed in the same position, with the polar head facing the water environment and the non-polar tail facing the air environment. Similarly, Chen Yijian, et al. [26] used the MD simulation method to study the behavior characteristics of the double-chain anionic surfactant sodium 1-alkyl - decyl sulfonate at the gas/liquid interface and also placed the surfactant molecules on the upper and lower sides of the water molecular layer.

Results and discussion

Density profile of Triton X molecules at the interface

In the studies of Liu, et al. [27] and Parra, et al. [12], the distribution of atoms, ions, or polar groups in different positions of the surfactant molecules under study on the water surface was determined by calculating the density profile along the Z-axis. In this paper, the density distribution of TX molecules on the interface was characterized by calculating the number densities of O atoms at different positions in three TX molecules and those of tail carbon and water molecules dependent on the Z axis, as shown in Figures 1,2.

As can be seen from the two diagrams, the O atom and the tail carbon atom in the TX-5 and TX-114 molecules are both in water and on the surface of the water. This phenomenon is shown at both the upper and lower interfaces. Most of the tail carbon atoms in the TX-100 molecules at the upper interface were exposed to air, while the rest of the O atoms and the atoms studied in the TX-100 molecules at the lower interface were immersed in the water. This is consistent with Fainerman, et al. [13] 's conclusion that the adsorption capacity of TX-100 at the air/water interface is so small that all PEO chains can be located in the surface layer. The number density of O atoms in the polar head hydroxyl group of TX molecules at the upper and lower interfaces is lower than that of other O atoms in the water, and this phenomenon occurs in all three systems. In addition, the number of water molecules on the interface of the three systems is greatly reduced, and the inflection points of decline correspond to the peaks of O atoms in different positions of TX molecules, which means that polar O atoms

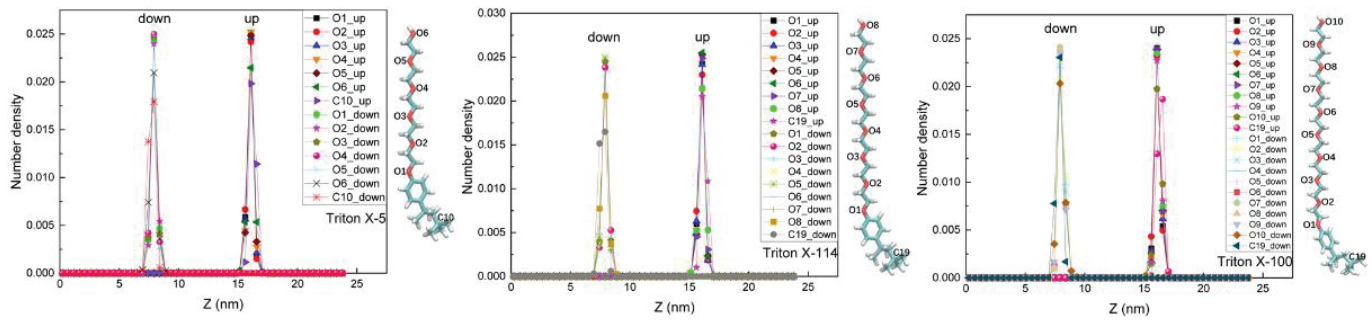


Figure 1: The O atoms and tail quaternary carbon at different positions in the TX molecule depend on the number density of the Z axis Note1. See the molecular diagram on the right for the labels of each O atom and tail quaternary carbon atom.

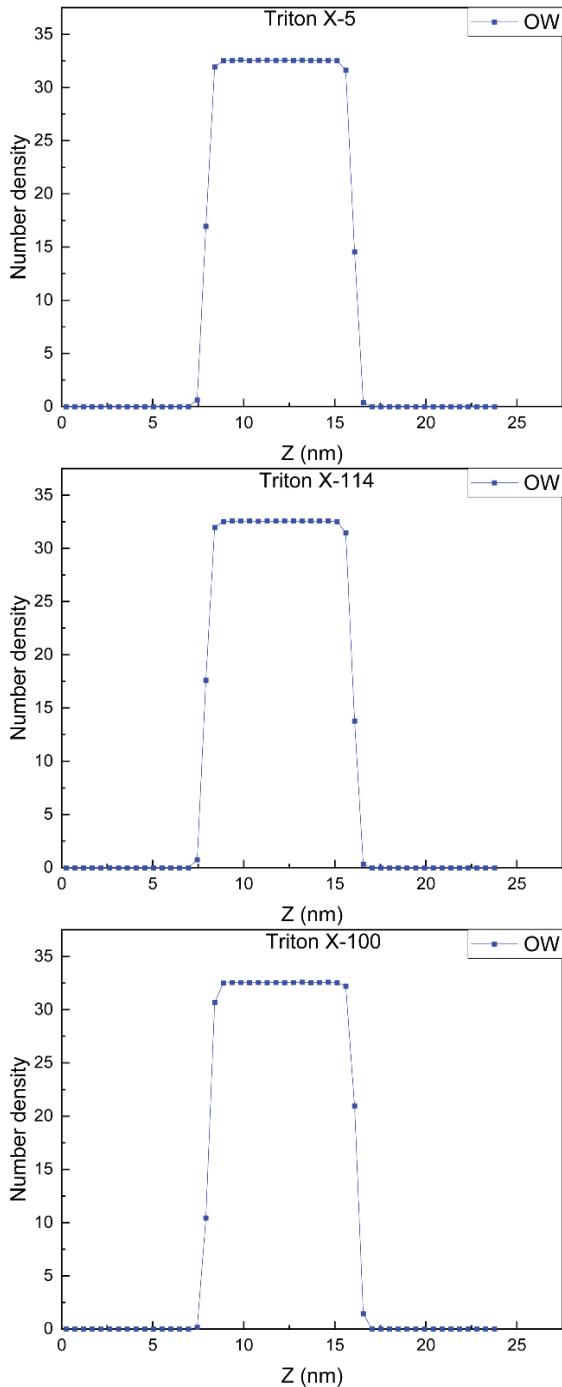


Figure 2: The O atom in the water molecule depends on the number density of the Z axis.

occupy a certain spatial position in the water surface. This result is similar to the simulation result obtained by Parra, et al. [12] that the existence of TX-100 at the air/water interface reduces the interface thickness of the water surface. In addition, the number density peaks of these atoms selected in the three TX molecular systems appear in very uniform positions, and the number density peaks of these atoms selected in each system are basically the same in the upper and lower interfaces, about 0.025.

Structure of Triton X molecular chain at the interface

The chain structure of surfactant molecules is usually characterized by order parameters, chain length, chain orientation, and Gauche defects. In this study, these indicators were measured to characterize the structure of three TX molecular chains at the air/water interface.

Order parameter: In order to characterize the order degree of TX molecules on the interface, the order parameters of C atoms in different positions of TX molecules were calculated in this paper. One of the C atoms with similar chemical environments was selected for study, as shown in Figure 3. The order parameters are calculated using this formula.

$$S_Z = \frac{3 \langle \cos^2 \theta_Z \rangle - 1}{2}$$

Where, is the included Angle between the Z-axis and the molecular axis of the simulated box, defined as the vector from C_{i-1} to $C_i + 1$. The mean value over time is shown in parentheses. The range of the order parameter is $[-1/2, 1]$. The larger the value, the higher the disorder of the chain (the more parallel to the z-axis), and the smaller the value, the more ordered (the more perpendicular to the z-axis). In the case of isotropic orientation, the value is zero [27]. As shown in the Figure, the chain order degree of TX-5, TX-114, and TX-100 molecules all showed a similar change trend. On the whole, TX molecules were relatively ordered on the interface and were almost perpendicular to the Z axis. The order parameter values of the three systems are TX-5, TX-114, and TX-100.

Length of surfactant chain: The length of the TX molecular chain is one of the basic characteristics of chain structure. This section determines the distance between the O atom at different positions in the TX molecule and the H atom in

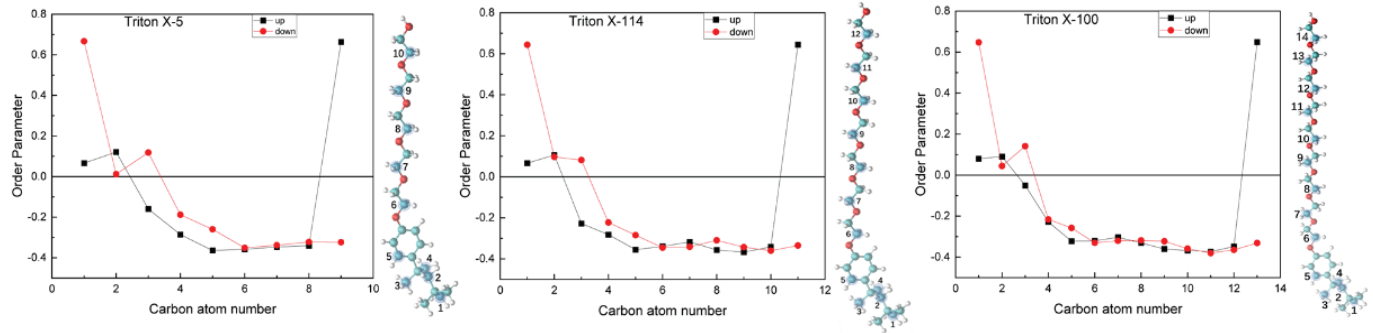


Figure 3: The order parameters of C atoms at different positions in TX-5, TX-114, and TX-100 molecules, see the molecular diagram on the right for the labels of C atoms at different positions.

the polar head hydroxyl group relative to the C atom in the terminal methyl group, as shown in Figure 4. TX-5 molecules at the upper interface showed an upward trend from O1 to O4, a downward trend from O4 to O6, and a weak increase in H42, indicating that the molecular chain had obvious bending and presented a symmetrical chain structure. The TX-5 molecule in the lower interface increased significantly from O1 to O6. The TX-114 molecule showed a nearly uniform upward trend from O1 to O8. The length variation trend of the TX-100 molecule increases gradually in the upper interface but fluctuates to a certain extent in the lower interface. The same TX molecule has different lengths on both the upper and lower water surfaces. In addition, the length of the three TX molecules at the interface is smaller than that of A free molecule optimized by quantum chemistry (26.073 Å for TX-5, 33.028 Å for TX-114, and 38.282 Å for TX-100).

Orientation of surfactant chain: In order to further explore the orientation of the TX molecular chain on the interface, this paper calculates the Angle between the Z axis and the vector from the O atom at different positions to the C atom of the terminal methyl group in the TX molecule, as shown in Figure 5. The angular distribution of TX-5 and TX-114 molecules increases at the upper interface as the O atom gets closer and closer to the polar head position, but the opposite is true at the lower interface. The Angle distribution of TX-100 molecules increased to a stable and then increased at the upper interface, and vice versa at the lower interface. The included Angle between the whole TX molecule (the vector where the O atom in the polar head hydroxyl group points to the terminal C atom) and the Z axis is greater than 80° in the three systems, which is consistent with the conclusion obtained in section 3.2.1 that the TX molecule is almost perpendicular to the Z axis.

Gauche defects: In order to further characterize the conformation of the TX molecular chain on the interface, this paper explored by calculating the probability distribution of gauche dihedral Angle in the TX molecule (Figure 6). As can be seen from the Figure, the probability value of gauche in the three systems decreases according to the sequence TX-100>TX-5>TX-114, indicating that the TX-100 molecule is the most stable on the interface. It is worth noting that the probability value of gauche in each system presents a

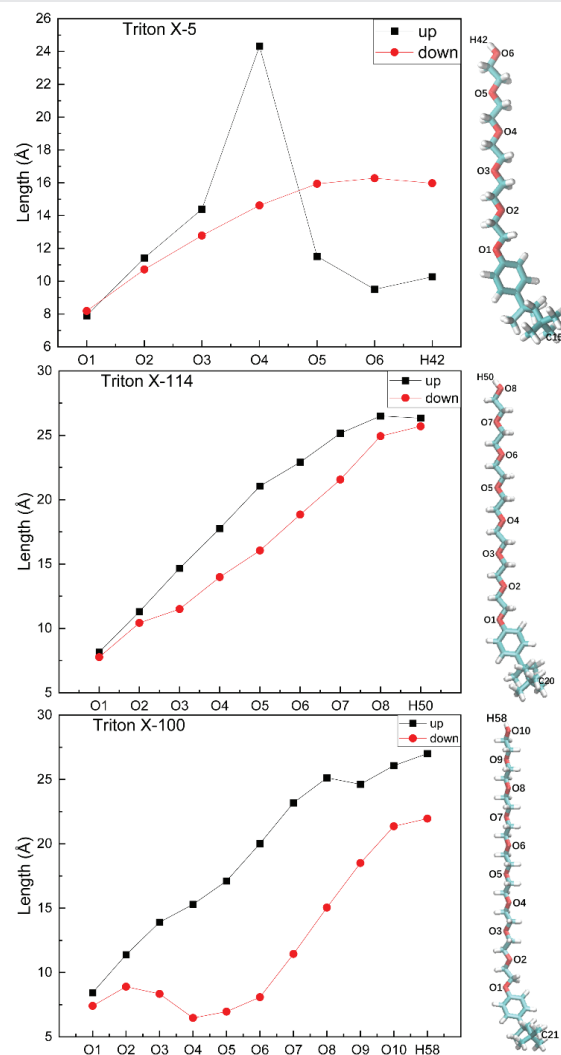


Figure 4: The distance between the O atom at different positions in TX-5, TX-114, and TX-100 molecules and the H atom in the polar head hydroxyl group relative to the C atom in the terminal methyl group Note1. See the molecular diagram on the right for the label of each atom.

wavy trend from the terminal C position to the polar head C position. The morphological structure of a single TX molecule at the air/water interface provides a certain reference for the morphological and structural characteristics of multiple TX molecules at the interface.

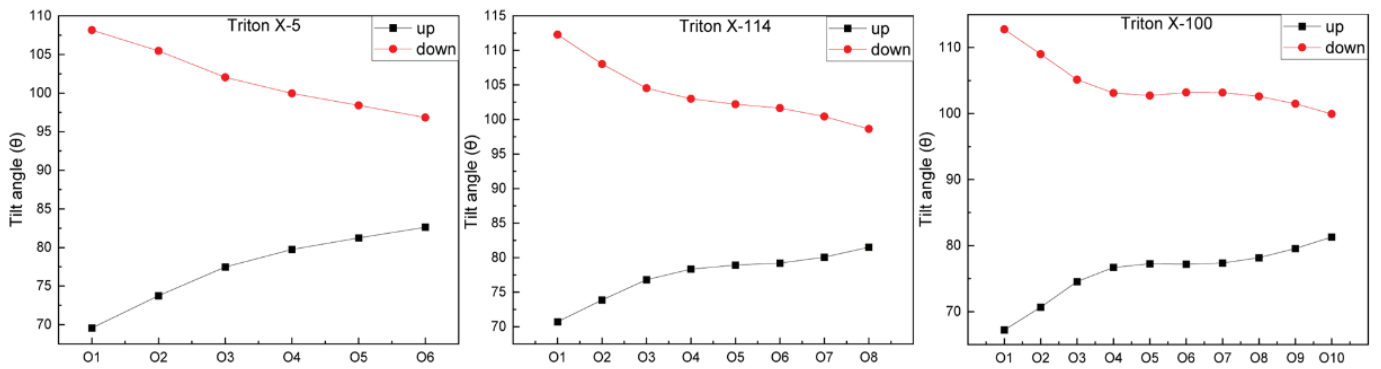


Figure 5: The angle between the vector from the O atom at different positions in the TX molecule to the C atom at the terminal methyl group and the Z axis Note1. The label of each atom is shown in the molecular diagram on the right side of Figure 4.

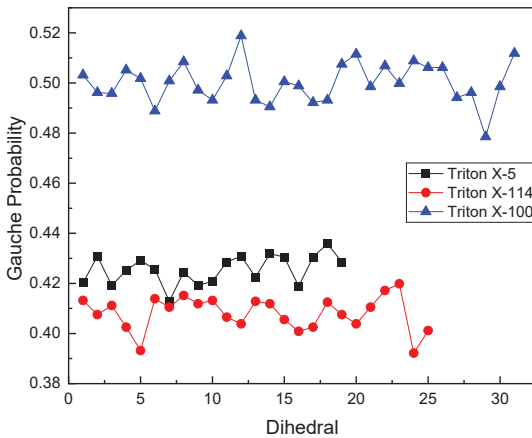


Figure 6: The gauche probability distribution function at position C.

Interaction between TX molecules and water on the interface

In this section, the hydration number, hydrogen bond number, and hydrogen bond relaxation time of atoms in different positions of three TX molecules were calculated to characterize the interaction of each TX molecule with water at the air/water interface. In order to increase the reliability of the simulation results, the same TX molecule's interaction with water at the upper and lower interfaces was also characterized in this paper.

Hydration number: In this paper, the hydration number of C and O atoms in different positions of TX-5, TX-114 and TX-100 surfactant molecules was calculated to characterize the interaction between TX molecules and water at the interface. One of the C atoms with a similar chemical environment is selected for study, as shown in Figure 7. The hydration number is obtained by calculating the integral of the Radial Distribution Function (RDF) of the selected water molecules around the C or O atom in the range of 0.35 nm [28,29]. As shown in the Figure, the hydration number of the three is basically the same. The hydration number of the octyl chain in the whole TX molecule is the lowest, all of which are less than 0.5, the hydration number of the benzene ring increases, and the hydration number of the PEO chain shows an obvious zigzag trend, that is, the hydration number of the O atom in each EO unit is much larger than that

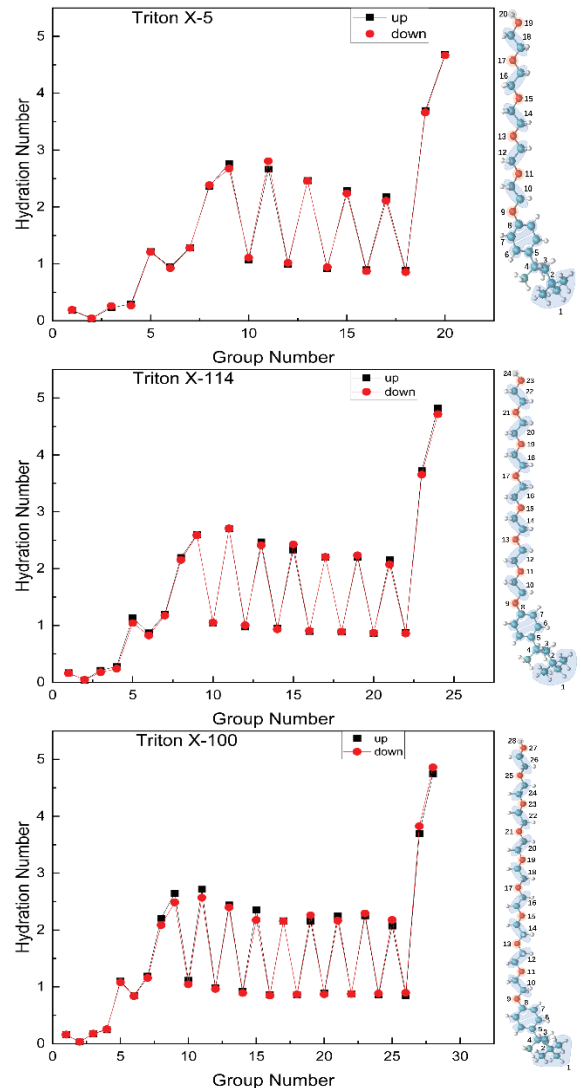


Figure 7: The hydration number of C atoms and O atoms at different positions in TX-5, TX-114, and TX-100 surfactant molecules. Note1: The Triton X molecular diagram on the right describes the atoms corresponding to each number, in which the dark green ball represents the C atom, the red ball represents the O atom, and the gray-white ball represents the H atom.

of the C atom, and their value is not more than 3. The hydration number of the polar head hydroxyl group reached the maximum (>8), which was largely due to the different steric hindrances

of atoms at different positions. This is similar to the trend of hydration number of the three TX micelles described in section 3.3.1. In addition, the hydration number of the EO unit in the TX-5 molecule decreases as it gradually approaches the polar head, and the hydration number of the EO unit in the TX-114 and TX-100 molecules fluctuates slightly. This phenomenon is due to the different distribution of TX molecules in water, the different conformation of the chains, and the different amounts of contact with water molecules [30–40]. It can be seen that the three TX molecules interact strongly with water, especially the hydration number of the PEO chain is significantly higher than that of the PEO chain in the micellar formation, that is, a single TX molecule is not easy to bubble at the air/water interface and its bubble stability is relatively low.

Hydrogen bond number: The geometric criterion for the existence of hydrogen bonds used in this paper is that the distance between donor and recipient pairs is within 3.5 Å, and the Angle between hydroxyl and oxygen atoms is less than or equal to 30°. Figure 8 shows that the hydrogen bond number of O atoms at different positions of the three systems is “small at both ends and large in the middle”. Moreover, the hydrogen bond number of the O atom in the middle of TX-114 and TX-100 molecules fluctuates significantly, which is similar to the trend of the hydration number of the O atom in Section 3.3.1. Surprisingly, the hydrogen bond number of O atoms in the polar head hydroxyl group decreases significantly. This means that very few of the water molecules it mixes with can form hydrogen bonds with it. In the TX-5 system, the hydrogen bond number of the O1 atom is the lowest, about 0.3, and the hydrogen bond number of the O2 atom increases significantly, reaching 0.475. Then, the hydrogen bond number of the O6 atom decreases, reaching 0.31. In the TX-114 system, the O1 atom also has the lowest hydrogen bond number, about 0.29, and then the hydrogen bond number increases significantly, reaching 0.46 for the O2 atom and 0.3 for the O8 atom. In the TX-100 system, the hydrogen bond number of the O1 atom is 0.27–0.3 and then the hydrogen bond number increases significantly, reaching 0.44 to the O2 atom, and the hydrogen bond number of the O10 atom is about 0.3 [41–80].

Hydrogen bond relaxation time: In order to further analyze the hydrogen bond kinetic properties of TX molecules at the interface, the relaxation times of hydrogen bonds between

O atoms and water molecules at different positions in TX molecules and between the outermost hydroxyl group and O atoms in water molecules were calculated (Figure 9). As can be seen from the Figure, the decay curves of the three systems gradually become gentle when they reach 10 ps. Among them, the decay curves of the outermost hydroxyl group and the O atom in the water molecule of the TX-5 and TX-114 systems decline the fastest, followed by that of the polar head O atom and the water molecule. In the TX-100 system, the decay rates of the two corresponding decay curves are similar and the fastest, indicating that it is difficult for polar head O atoms to form hydrogen bonds with water molecules, which is consistent with the result in section 3.3.2 that the number of hydrogen bonds of polar head O atoms is very low. In addition, the decay curve of the O1 atom connected with the benzene ring and water molecule also showed a very fast decay rate. The decay rate of the decay curve between the O atom and the water molecule in the remaining position is relatively slower, so the number of hydrogen bonds formed is higher [81–132].

Conclusion

The structure of three TX molecules with different PEO chain lengths at the air/water interface was studied by molecular dynamics simulation. Simulation results showed that the number density of O atoms in the polar head hydroxyl group of TX-5, TX-114, and TX-100 molecules was lower than that of other O atoms and occupied a certain spatial position in the water surface. In addition, the three TX molecules are relatively ordered on the interface, and all are almost perpendicular to the Z axis. The Angle between the TX molecule and the Z axis is greater than 80 degrees in all three systems. Each of the three TX chains has a different structure at the air/water interface and is somewhat shorter in length. The probability value of gauche in the three systems decreased by this sequence TX-100>TX-5~TX-114. Notably, the number of hydrogen bonds of the O atom in the polar head hydroxyl group decreased significantly, meaning that very few water molecules could form hydrogen bonds with it. This study has a certain guiding significance for better control of the foaming property and foam stability of TX molecules. In addition, the study of TX molecules at the air/water interface provides a certain reference for the exploration of TX molecules forming micelles when they reach the critical micelle concentration.

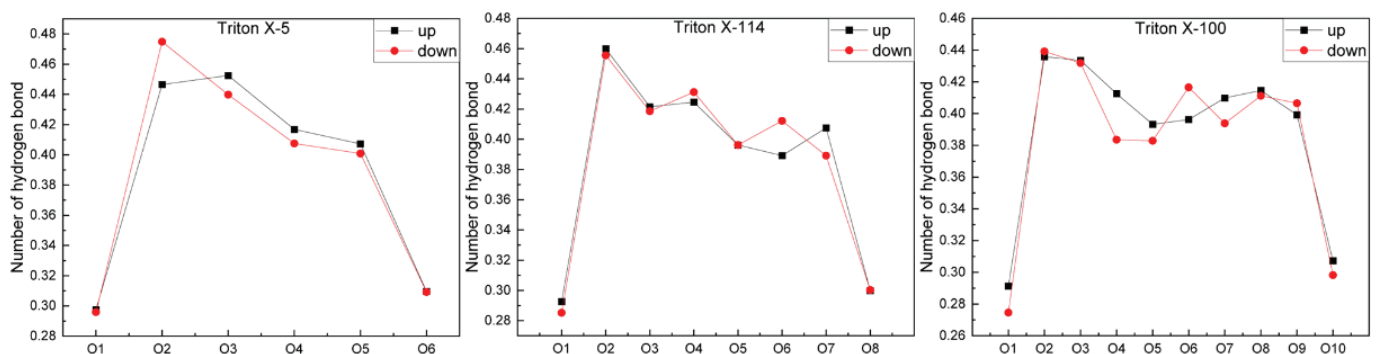


Figure 8: The number of hydrogen bonds formed between O atoms at different positions in TX-5, TX-114, and TX-100 molecules and water molecules, the labels of each O atom are shown in the molecular schematic diagram in Figure 1.

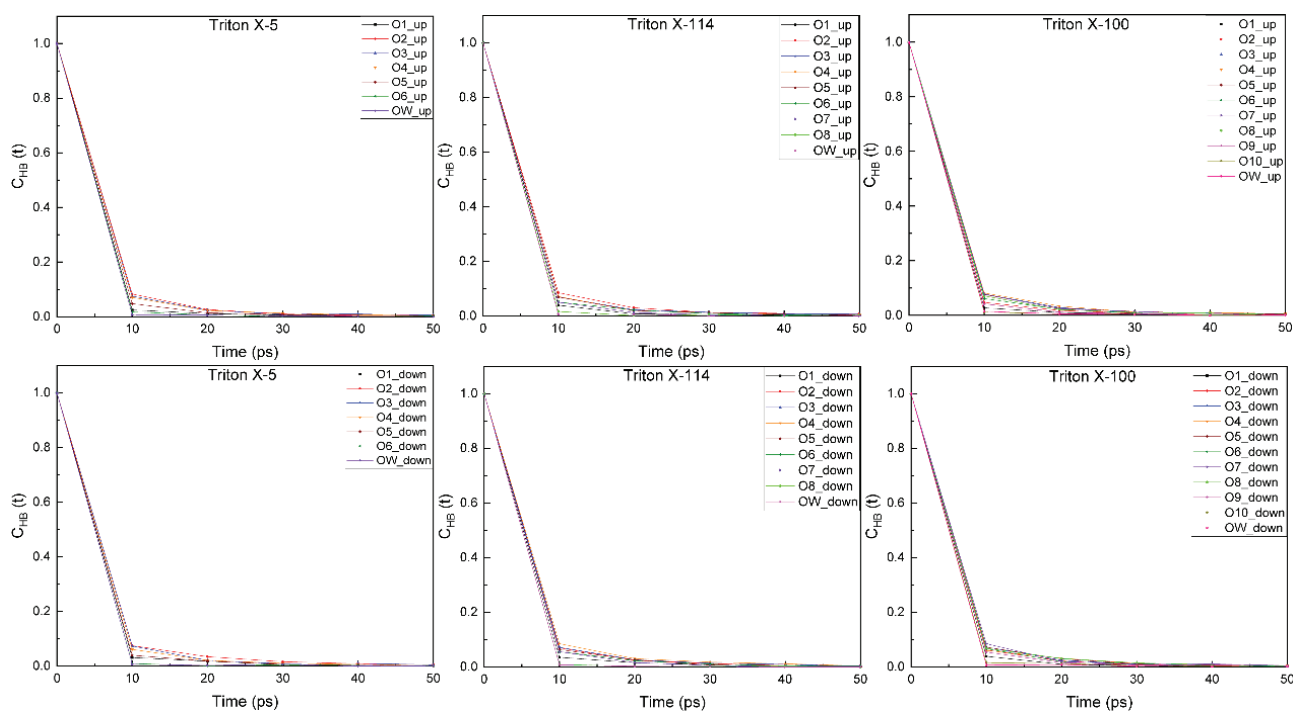


Figure 9: The hydrogen bond relaxation time between O atoms at different positions in TX-5, TX-114, and TX-100 molecules and between the outermost hydroxyl group and O atoms in water molecules, the labels of each O atom are the same as the molecular schematic diagram in Figure 1.

References

- Azum N, Rub MA, Khan SB. Complexation behavior of mixed monolayer/mixed micelle formation between cationic noble surfactant-nonionic conventional surfactant in the presence of biocompatible polymer. *Journal of Molecular Liquids*. 2014; 199: 495-500.
- Shao Y, Li Y, Cao X. Effect of inorganic positive ions on the adsorption of surfactant Triton X-100 at quartz/solution interface. *Science in China Series B: Chemistry*. 2008; 51(10): 918-927.
- Wei XF, Liu HZ. Relationship between foaming properties and solution properties of protein/nonionic surfactant mixtures. *Journal of Surfactants and Detergents*. 2000; 3(4): 491-495.
- Coke M, Wilde PJ, Russell EJ. The influence of surface composition and molecular diffusion on the stability of foams formed from protein/surfactant mixtures. *Journal of Colloid and Interface Science*. 1990; 138(2): 489-504.
- Murray BS, Ventura A, Lallemand C. Dilatational rheology of protein+ non-ionic surfactant films at air–water and oil–water interfaces. *Colloids and Surfaces A: Physicochemical and Engineering Aspects*. 1998; 143(2-3): 211-219.
- Patino JMR, Niño RR, Gómez JMÁ. Interfacial and foaming characteristics of protein–lipid systems. *Food Hydrocolloids*. 1997; 11(1): 49-58.
- Németh Z, Rácz G, Koczó K. Antifoaming action of polyoxyethylene-polyoxypropylene-polyoxyethylene-type triblock copolymers on bsa foams. *Colloids and Surfaces A: Physicochemical and Engineering Aspects*. 1997; 127(1-3): 151-162.
- Kanokkarn P, Shiina T, Santikunaporn M. Equilibrium and dynamic surface tension in relation to diffusivity and foaming properties: effects of surfactant type and structure. *Colloids and Surfaces A: Physicochemical and Engineering Aspects*. 2017; 524: 135-142.
- Beneventi D, Carre B, Gandini A. Role of surfactant structure on surface and foaming properties. *Colloids and Surfaces A: Physicochemical and Engineering Aspects* 2001; 189(1-3): 65-73.
- Tamura T, Takeuchi Y, Kaneko Y. Influence of surfactant structure on the drainage of nonionic surfactant foam films. *Journal of Colloid and Interface Science* 1998; 206(1): 112-121.
- Rosen M J, Zhu Z H, Gu B, et al. Relationship of structure to properties of surfactants. 14. Some n-alkyl-2-pyrrolidones at various interfaces. *Langmuir*. 1988; 4(6): 1273-1277.
- Parra J G, Iza P, Dominguez H, et al. Effect of Triton X-100 surfactant on the interfacial activity of ionic surfactants sds, ctab and sdbs at the air/water interface: a study using molecular dynamic simulations. *Colloids and Surfaces A: Physicochemical and Engineering Aspects*. 2020; 603: 125284.
- Fainerman V, Makievski A, Joos P. Adsorption kinetics of octylphenyl ethers of poly (ethylene glycol)s on the solution-air interface. *Colloids and Surfaces A: Physicochemical and Engineering Aspects*. 1994; 90(2-3): 213-224.
- Azum N, Rub M A, Asiri A M, et al. Micellar and interfacial properties of amphiphilic drug–non-ionic surfactants mixed systems: surface tension, fluorescence and uv–vis studies. *Colloids and Surfaces A: Physicochemical and Engineering Aspects*. 2017; 522: 183-192.
- Agneta M, Zhaomin L, Chao Z, et al. Investigating synergism and antagonism of binary mixed surfactants for foam efficiency optimization in high salinity. *Journal of Petroleum Science and Engineering*. 2019; 175: 489-494.
- Li Y, He X, Cao X, et al. Molecular behavior and synergistic effects between sodium dodecylbenzene sulfonate and Triton X-100 at oil/water interface. *Journal of Colloid and Interface Science*. 2007; 307(1): 215-220.
- Tarek M, Tobias D J, Klein M L. Molecular dynamics simulation of tetradecyltrimethylammonium bromide monolayers at the air/water interface. *The Journal of Physical Chemistry*. 1995; 99(5): 1393-1402.
- Xu C, Mandal T, Larson R G, et al. A molecular dynamics simulation of the structure of sodium lauryl ether sulfate and poly(vinyl alcohol) at the air/water interface. *Colloids and Surfaces A: Physicochemical and Engineering Aspects*. 2019; 563: 84-94.
- Chanda J, Bandyopadhyay S. Molecular dynamics study of a surfactant



- monolayer adsorbed at the air/water interface. *Journal of Chemical Theory and Computation*. 2005; 1(5): 963-971.
20. Frisch MJ, Trucks GW, Schlegel HB. *Gaussian 09 Rev. A.03[CP]*. Inc, Wallingford, CT, 2009.
21. Koziara KB, Stroet M, Malde AK. Testing and validation of the automated topology builder (atb) version 2.0: prediction of hydration free enthalpies. *Journal of Computer-Aided Molecular Design*. 2014; 28(3): 221-233.
22. Malde AK, Zuo L, Breeze M. An automated force field topology builder (atb) and repository: version 1.0. *Journal of Chemical Theory and Computation*. 2011; 7(12): 4026-4037.
23. Abraham M, Murtola T, Schulz R. Gromacs: high performance molecular simulations through multi-level parallelism from laptops to supercomputers. *SoftwareX*. 2015; 1-2: 19-25.
24. Hess B, Bekker H, Berendsen HJC. Lincs: a linear constraint solver for molecular simulations. *Journal of Computational Chemistry*. 1997; 18(12): 1463-1472.
25. Humphrey W, Dalke A, Schulten K. Vmd: visual molecular dynamics. *Journal of Molecular Graphics*. 1996; 14(1): 33-38.
26. Chen Yijian, Zhou Hongtao, Ge Jijiang. Aggregation behavior of double-chain anionic surfactant sodium 1-alkyl-decylsulfonate at air/liquid interface: Molecular dynamics simulation study. *Physical Chemistry Acta*. 2017; 33(06): 1214-1222.
27. Liu G, Li R, Wei Y. Molecular dynamics simulations on tetraalkylammonium interactions with dodecyl sulfate micelles at the air/water interface. *Journal of Molecular Liquids*. 2016; 222: 1085-1090.
28. Chun BJ, Choi JI, Jang SS. Molecular dynamics simulation study of sodium dodecyl sulfate micelle: water penetration and sodium dodecyl sulfate dissociation. *Colloids and Surfaces A: Physicochemical and Engineering Aspects*. 2015; 474: 36-43.
29. Gao J, Ge W, Hu G. From homogeneous dispersion to micelles: molecular dynamics simulation on the compromise of the hydrophilic and hydrophobic effects of sodium dodecyl sulfate in aqueous solution. *Langmuir*. 2005; 21(11): 5223-5229.
30. Yazdi AS. Surfactant-based extraction methods. *TRAC Trends in Analytical Chemistry*. 2011; 30(6): 918-929.
31. Lawrence MJ. Surfactant systems: their use in drug delivery. *Chemical Society Reviews*. 1994; 23(6): 417-424.
32. Cullum D. *Introduction to surfactant analysis*. Springer, 1994.
33. Attwood D. *Surfactant systems: their chemistry, pharmacy and biology*. Springer Science & Business Media, 2012.
34. Zhang L, Chai X, Sun P. The study of the aggregated pattern of tx100 micelle by using solvent paramagnetic relaxation enhancements. *Molecules*. 2019; 24(9), 1649.
35. Brown W, Rymden R, Van Stam J. Static and dynamic properties of nonionic amphiphile micelles: Triton X-100 in aqueous solution. *The Journal of Physical Chemistry*. 1989; 93(6): 2512-2519.
36. Robson RJ, Dennis EA. The size, shape, and hydration of nonionic surfactant micelles. Triton X-100. *The Journal of Physical Chemistry*. 1977; 81(11): 1075-1078.
37. Ishkhanyan H, Rhys NH, Barlow DJ. Impact of drug aggregation on the structural and dynamic properties of Triton X-100 micelles. *Nanoscale*. 2022; 14(14): 5392-5403.
38. Durrant JD, Mccammon JA. Molecular dynamics simulations and drug discovery. *BMC Biology*. 2011; 9(1): 71.
39. Hospital A, Goñi JR, Orozco M. Molecular dynamics simulations: Advances and applications. *Advances and Applications in Bioinformatics and Chemistry*. 2015; 8: 37-47.
40. Hollingsworth SA, Dror RO. Molecular dynamics simulation for all. *Neuron*. 2018; 99(6): 1129-1143.
41. Van Gunsteren WF, Mark AE. Validation of molecular dynamics simulation. *The Journal of Chemical Physics*. 1998; 108(15): 6109-6116.
42. Yan H, Cui P, Liu CB. Molecular dynamics simulation of pyrene solubilized in a sodium dodecyl sulfate micelle. *Langmuir*. 2012; 28(11): 4931-4938.
43. Huan H, Hongxin N, Xuechao Y. Solubilization of flavonol glycosides by sodium lauryl sulfate based on molecular dynamics and its effect on pharmacokinetics in vivo. *Drug Evaluation Studies*. 2021; 44(1): 25-30.
44. Wang Y, Meng X, Che B. The effect of molecular dynamics simulation temperature on the structure of ctab/sa micelles. *Journal of Liaocheng University (Natural Science Edition)*. 2018; 31(4): 99-103.
45. Lebecque S, Crowet J M, Nasir MN. Molecular dynamics study of micelles properties according to their size. *Journal of Molecular Graphics and Modelling*. 2017; 72: 6-15.
46. Karaborni S, Van Os NM, Esselink K. Molecular dynamics simulations of oil solubilization in surfactant solutions. *Langmuir*. 1993; 9(5): 1175-1178.
47. Bruce CD, Berkowitz ML, Perera L. Molecular dynamics simulation of sodium dodecyl sulfate micelle in water: Micellar structural characteristics and counterion distribution. *The Journal of Physical Chemistry B*. 2002; 106(15): 3788-3793.
48. Shelley J, Watanabe K, Klein ML. Simulation of a sodium dodecylsulfate micelle in aqueous solution. *International Journal of Quantum Chemistry*. 1990; 38(S17): 103-117.
49. Wei Y, Wang H, Liu G. A molecular dynamics study on two promising green surfactant micelles of choline dodecyl sulfate and laurate. *RSC advances*. 2016; 6(87): 84090-84097.
50. Mackerell AD. Molecular dynamics simulation analysis of a sodium dodecyl sulfate micelle in aqueous solution: decreased fluidity of the micelle hydrocarbon interior. *The Journal of Physical Chemistry*. 1995; 99(7): 1846-1855.
51. Yoshii N, Iwahashi K, Okazaki SA. Molecular dynamics study of free energy of micelle formation for sodium dodecyl sulfate in water and its size distribution. *The Journal of Chemical Physics*. 2006; 124(18): 184901.
52. Shang BZ, Wang Z, Larson RG. Effect of headgroup size, charge, and solvent structure on polymer-micelle interactions, studied by molecular dynamics simulations. *The Journal of Physical Chemistry B*. 2009; 113(46): 15170-15180.
53. Koneva AS, Ritter E, Anufrikov YA. Mixed aqueous solutions of nonionic surfactants Brij 35/Triton X-100: micellar properties, solutes' partitioning from micellar liquid chromatography and modelling with cosmomic. *Colloids and Surfaces A: Physicochemical and Engineering Aspects*. 2018; 538: 45-55.
54. Guruge AG, Warren DB, Benameur H. Aqueous phase behavior of the peo-containing non-ionic surfactant C12E6: a molecular dynamics simulation study. *Journal of Colloid and Interface Science*. 2021; 588: 257-268.
55. Winger M, De Vries AH, Van Gunsteren WF. Force-field dependence of the conformational properties of α,ω -dimethoxypolyethylene glycol. *Molecular Physics*. 2009; 107(13): 1313-1321.
56. Fuchs PFJ, Hansen HS, Hünenberger PH. A gromos parameter set for vicinal diether functions: properties of polyethyleneoxide and polyethyleneglycol. *Journal of Chemical Theory and Computation*. 2012; 8(10): 3943-3963.



57. De Nicola A, Kawakatsu T, Rosano C. Self-assembly of Triton X-100 in water solutions: a multiscale simulation study linking mesoscale to atomistic models. *Journal of Chemical Theory and Computation*. 2015; 11(10): 4959-4971.
58. Murakami W, De Nicola A, Oya Y. Theoretical and computational study of the sphere-to-rod transition of Triton X-100 micellar nanoscale aggregates in aqueous solution: implications for membrane protein purification and membrane solubilization. *ACS Applied Nano Materials*. 2021; 4(5): 4552-4561.
59. Farafonov V, Lebed A, Khimenko N. Molecular dynamics study of an acid-base indicator dye in Triton X-100 non-ionic micelles. *Voprosy khimii i khimicheskoi tekhnologii*. 2020; 1: 97-103.
60. Ritter E, Yordanova D, Gerlach T. Molecular dynamics simulations of various micelles to predict micelle water partition equilibria with cosmomic: influence of micelle size and structure. *Fluid Phase Equilibria*. 2016; 422: 43-55.
61. Yordanova D, Smirnova I, Jakobtorweihen S. Molecular modeling of Triton X micelles: force field parameters, self-assembly, and partition equilibria. *Journal of Chemical Theory and Computation*. 2015; 11(5): 2329-2340.
62. Ishkhanyan H, Ziolk RM, Barlow DJ. Nsaid solubilisation promotes morphological transitions in Triton X-114 surfactant micelles. *Journal of Molecular Liquids*. 2022; 356: 119050.
63. Pacheco-Blas MDA, Vicente L. Molecular dynamics study of the behaviour of surfactant Triton X-100 in the extraction process of Cd²⁺. *Chemical Physics Letters*. 2020; 739: 136920.
64. Pizzirusso A, De Nicola A, Sevink GJA. Biomembrane solubilization mechanism by Triton X-100: a computational study of the three stage model. *Physical Chemistry Chemical Physics*. 2017; 19(44): 29780-29794.
65. Pryde JG. Triton X-114: a detergent that has come in from the cold. *Trends in Biochemical Sciences*. 1986; 11(4): 160-163.
66. Paradies HH. Shape and size of a nonionic surfactant micelle. Triton X-100 in aqueous solution. *The Journal of Physical Chemistry*. 1980; 84(6): 599-607.
67. Yuan HZ, Cheng GZ, Zhao S. Conformational dependence of Triton X-100 on environment studied by 2D Noesy and 1H NMR relaxation. *Langmuir*. 2000; 16(7): 3030-3035.
68. Denkova PS, Lokeren LV, Verbruggen I. Self-aggregation and supramolecular structure investigations of Triton X-100 and sdp2s by noesy and diffusion ordered nmr spectroscopy. *The Journal of Physical Chemistry B*. 2008; 112(35): 10935-10941.
69. Mote US, Patil SR, Kolekar GB. Fluorescence spectroscopic studies on interaction between carprofen and Triton X-100 micelle. *Journal of Molecular Liquids*. 2010; 157(2): 102-104.
70. Göktürk S, Çalışkan E, Talman R Y, et al. A study on solubilization of poorly soluble drugs by cyclodextrins and micelles: complexation and binding characteristics of sulfamethoxazole and trimethoprim[J]. *The Scientific World Journal*, 2012, 2012: 718791.
71. Duarte ARC, Coimbra P, De Sousa HC. Solubility of flurbiprofen in supercritical carbon dioxide. *Journal of Chemical & Engineering Data*. 2004; 49(3): 449-452.
72. Barden J, Edwards JE, Mcquay HJ. Oral valdecoxib and injected parecoxib for acute postoperative pain: a quantitative systematic review. *BMC Anesthesiology*. 2003; 3(1): 1.
73. Ullah I, Baloch MK, Durrani GF. Solubility of nonsteroidal anti-inflammatory drugs (nsaids) in aqueous solutions of non-ionic surfactants[J]. *Journal of Solution Chemistry*. 2011; 40(7): 1341-1348.
74. Ullah I, Baloch MK, Niaz S. Solubilizing potential of ionic, zwitterionic and nonionic surfactants towards water insoluble drug flurbiprofen. *Journal of Solution Chemistry*. 2019; 48(11): 1603-1616.
75. Rub MA, Khan F, Sheikh MS. Tensiometric, fluorescence and 1h nmr study of mixed micellization of non-steroidal anti-inflammatory drug sodium salt of ibuprofen in the presence of non-ionic surfactant in aqueous/urea solutions[J]. *The Journal of Chemical Thermodynamics*. 2016; 96: 196-207.
76. He M, Zheng W, Wang N. Molecular dynamics simulation of drug solubilization behavior in surfactant and cosolvent injections [J/OL] 2022; 14(11):10.3390/pharmaceutics14112366
77. Liu Y, Liu M, Yan H. Enhanced solubility of bisdemethoxycurcumin by interaction with tween surfactants: spectroscopic and coarse-grained molecular dynamics simulation studies. *Journal of Molecular Liquids*. 2021; 323: 115073.
78. Chang CH, Franses EI. Adsorption dynamics of surfactants at the air/water interface: a critical review of mathematical models, data, and mechanisms. *Colloids and Surfaces A: Physicochemical and Engineering Aspects*. 1995; 100: 1-45.
79. Szymczyk K, Jańczuk B. The adsorption at solution-air interface and volumetric properties of mixtures of cationic and nonionic surfactants. *Colloids and Surfaces A: Physicochemical and Engineering Aspects*. 2007; 293(1): 39-50.
80. Pawliszak P, Zawala J, Ulaganathan V. Interfacial characterisation for flotation: 2. Air-water interface. *Current Opinion in Colloid & Interface Science*. 2018; 37: 115-127.
81. Janczuk B, Bruque JM, Gonzalez-Martin ML. The adsorption of Triton X-100 at the air-aqueous solution interface. *Langmuir*. 1995; 11(11): 4515-4518.
82. Wang L, Liu R, Hu Y. Adsorption of mixed dda/naol surfactants at the air/water interface by molecular dynamics simulations. *Chemical Engineering Science*. 2016; 155: 167-174.
83. Wang L, Hu Y, Liu R. Synergistic adsorption of dda/alcohol mixtures at the air/water interface: a molecular dynamics simulation. *Journal of Molecular Liquids*. 2017; 243: 1-8.
84. Barzykin AV, Tachiya M. Interpretation of passive permeability measurements on lipid-bilayer vesicles. Effect of fluctuations. *Biochimica et Biophysica Acta (BBA) – Biomembranes*. 1997; 1330(2): 121-126.
85. Azum N, Rub M A, Azim Y. Micellar and spectroscopic studies of amphiphilic drug with nonionic surfactant in the presence of ionic liquids. *Journal of Molecular Liquids*. 2020; 315.
86. Jaiswal S, Mondal R, Paul D. Investigating the micellization of the triton-x surfactants: a non-invasive fluorometric and calorimetric approach. *Chemical Physics Letters*. 2016; 646: 18-24.
87. Abu-Ghunmi L, Badawi M, Fayyad M. Fate of Triton X-100 applications on water and soil environments: a review[J]. *Journal of Surfactants and Detergents*. 2014; 17(5): 833-838.
88. Molina-Bolívar JA, Aguiar J, Ruiz CC. Growth and hydration of Triton X-100 micelles in monovalent alkali salts: a light scattering study. *The Journal of Physical Chemistry B*. 2002; 106(4): 870-877.
89. Li M, Rharbi Y, Huang X. Small variations in the composition and properties of Triton X-100[J]. *Journal of Colloid and Interface Science*. 2000; 230(1): 135-139.
90. Thakkar K, Patel V, Ray D. Interaction of imidazolium based ionic liquids with Triton X-100 micelles: investigating the role of the counter ion and chain length. *RSC Advances*. 2016; 6(43): 36314-36326.
91. Kumbhakar M, Goel T, Mukherjee T. Role of micellar size and hydration on solvation dynamics: a temperature dependent study in triton-x-100 and brij-35 micelles. *The Journal of Physical Chemistry B*. 2004; 108(50): 19246-19254.
92. Ruiz CC, Molina-Bolívar JA, Aguiar J. Thermodynamic and structural studies of Triton X-100 micelles in ethylene glycol-water mixed solvents. *Langmuir*. 2001; 17(22): 6831-6840.



93. Kumbhakar M, Nath S, Mukherjee T. Solvation dynamics in triton-x-100 and triton-x-165 micelles: effect of micellar size and hydration. *The Journal of Chemical Physics*. 2004; 121(12): 6026-6033.
94. Fedyaeva OA, Poshelyuzhnaya EG. Dimensions and orientation of Triton X-100 micelles in aqueous solutions, according to turbidimetric data. *Russian Journal of Physical Chemistry A*. 2019; 93(12): 2559-2561.
95. Streltzyk K, Phillies GD. Temperature dependence of Triton X-100 micelle size and hydration. *Langmuir*. 1995; 11(1): 42-47.
96. Mandal A, Ray S, Biswas A. Physicochemical studies on the characterization of Triton X 100 micelles in an aqueous environment and in the presence of additives. *The Journal of Physical Chemistry*. 1980; 84(8): 856-859.
97. Phillies GD, Yambert JE. Solvent and solute effects on hydration and aggregation numbers of Triton X-100 micelles. *Langmuir*. 1996; 12(14): 3431-3436.
98. Phillies G D, Stott J, Ren S. Probe diffusion in the presence of nonionic amphiphiles: Triton X 100. *The Journal of Physical Chemistry*. 1993; 97(44): 11563-11568.
99. Qiao L, Easteal A J. Mass transport in Triton X series nonionic surfactant solutions: a new approach to solute-solvent interactions. *Colloid and Polymer Science*. 1996; 274(10): 974-980.
100. Rauf MA, Hisaindee S, Graham JP. Effect of various solvents on the absorption spectra of dithizone and dft calculations. *Journal of Molecular Liquids*. 2015; 211: 332-337.
101. Faramarzi S, Bonnett B, Scaggs CA. Molecular dynamics simulations as a tool for accurate determination of surfactant micelle properties. *Langmuir*. 2017; 33(38): 9934-9943.
102. Pal A, Pillania A. Modulations in surface and aggregation properties of non-ionic surfactant Triton X-45 on addition of ionic liquids in aqueous media. *Journal of Molecular Liquids*. 2017; 233: 243-250.
103. Stubičar N, Petres J. Micelle formation by tritons in aqueous solutions. *Croatica Chemica Acta*. 1981; 54(3): 255-266.
104. Biaselle CJ, Millar DB. Studies on Triton X-100 detergent micelles. *Biophysical Chemistry*. 1975; 3(4): 355-361.
105. Acosta E, Bisceglia M, Kurlat DH. Self-aggregation in aqueous Triton X-100 solutions near cmc. *Physics and Chemistry of Liquids*. 2005; 43(3): 269-275.
106. Phillies GDJ, Yambert JE. Solvent and solute effects on hydration and aggregation numbers of Triton X-100 micelles. *Langmuir*. 1996; 12(14): 3431-3436.
107. Giorgio G, Colafemmina G, Mavelli F. The impact of alkanes on the structure of Triton X100 micelles. *RSC advances*. 2016; 6(1): 825-836.
108. Valaulikar B, Manohar C. The mechanism of clouding in Triton X-100: the effect of additives. *Journal of Colloid and Interface Science*. 1985; 108(2): 403-406.
109. Yedgar S, Barenholz Y, Cooper V. Molecular weight, shape and structure of mixed micelles of Triton X-100 and sphingomyelin[J]. *Biochimica et Biophysica Acta (BBA)-Biomembranes*. 1974; 363(1): 98-111.
110. Allen DT, Saaka Y, Lawrence MJ. Atomistic description of the solubilisation of testosterone propionate in a sodium dodecyl sulfate micelle. *J Phys Chem B*. 2014; 118(46): 13192-13201.
111. Wei Y, Liu G, Wang Z. Molecular dynamics study on the aggregation behaviour of different positional isomers of sodium dodecyl benzenesulphonate. *RSC Advances*. 2016; 6(55): 49708-49716.
112. Liu G, Zhang H, Liu G. Tetraalkylammonium interactions with dodecyl sulfate micelles: a molecular dynamics study. *Phys Chem Chem Phys*. 2016; 18(2): 878-885.
113. Eisenhaber F, Lijnzaad P, Argos P. The double cubic lattice method: efficient approaches to numerical integration of surface area and volume and to dot surface contouring of molecular assemblies. *Journal of Computational Chemistry*. 1995; 16(3): 273-284.
114. Tang X, Koenig PH, Larson RG. Molecular dynamics simulations of sodium dodecyl sulfate micelles in water-the effect of the force field. *J Phys Chem B*. 2014; 118(14): 3864-3880.
115. Palazzesi F, Calvaresi M, Zerbetto F. A molecular dynamics investigation of structure and dynamics of sds and sdbs micelles. *Soft Matter*. 2011; 7: 9148-9156.
116. Palazzesi F, Calvaresi M, Zerbetto F. A molecular dynamics investigation of structure and dynamics of sds and sdbs micelles. *Soft Matter*. 2011; 7(19): 9148-9156.
117. Liu G, Zhang H, Liu G, Yuan S, Liu C. Tetraalkylammonium interactions with dodecyl sulfate micelles: a molecular dynamics study. *Phys Chem Chem Phys*. 2016 Jan 14;18(2):878-85. doi: 10.1039/c5cp05639j. PMID: 26646374.
118. Boese AD, Chandra A, Martin JML. From ab initio quantum chemistry to molecular dynamics: the delicate case of hydrogen bonding in ammonia. *The Journal of Chemical Physics*. 2003; 119(12): 5965-5980.
119. Pal S, Bagchi B, Balasubramanian S. Hydration layer of a cationic micelle, C10TAB: structure, rigidity, slow reorientation, hydrogen bond lifetime, and solvation dynamics. *The Journal of Physical Chemistry B*. 2005; 109(26): 12879-12890.
120. Song X, Zhang X, Peng J. Molecular dynamics study on the aggregation behaviours of platonic micelle in different nacl solutions. *Journal of Molecular Liquids*. 2022; 353: 118828.
121. Weifeng Z, Zhiwei Z, Wenliang K. Application progress of molecular dynamics simulation technology in self-assembled nano drug delivery system. *Acta Pharmaceutica*. 2023; 58(1): 118-126.
122. Allen DT, Saaka Y, Lawrence MJ, Lorenz CD. Atomistic description of the solubilisation of testosterone propionate in a sodium dodecyl sulfate micelle. *J Phys Chem B*. 2014 Nov 20;118(46):13192-201. doi: 10.1021/jp508488c. Epub 2014 Nov 7. PMID: 25343221.
123. Rub M A, Pulikkal A K, Azum N. The assembly of amitriptyline hydrochloride + Triton X-45 (non-ionic surfactant) mixtures: effects of simple salt and urea. *Journal of Molecular Liquids*. 2022; 356: 118997.
124. Fan X, Zhao X, Su W. Triton X-100-modified adenosine triphosphate-responsive siRNA delivery agent for antitumor therapy. *Molecular Pharmaceutics*. 17(10): 3696-3708.
125. Chakraborty H, Banerjee R, Sarkar M. Incorporation of NSAIDs in micelles: implication of structural switchover in drug-membrane interaction. *Biophys Chem*. 2003 May 1;104(1):315-25. doi: 10.1016/s0301-4622(02)00389-7. PMID: 12834850.
126. Day RO, Graham GG. Non-steroidal anti-inflammatory drugs (nsaids). *BMJ: British Medical Journal*. 2013; 346: f3195.
127. Tasaki Y, Yamamoto J, Omura T. Oxycam structure in non-steroidal anti-inflammatory drugs is essential to exhibit akt-mediated neuroprotection against 1-methyl-4-phenyl pyridinium-induced cytotoxicity. *European Journal of Pharmacology*. 2012; 676(1): 57-63.
128. Lindahl E, Abraham M, Hess B. Gromacs 2019 source code (2018). URL <https://doi.org/105281/zenodo,2022,2424363>.



129. Rahman A, Stillinger FH. Molecular dynamics study of liquid water. *The Journal of Chemical Physics*. 1971; 55(7): 3336-3359.
130. Parrinello M, Rahman A. Polymorphic transitions in single crystals: a new molecular dynamics method. *Journal of Applied Physics*. 1981; 52(12): 7182-7190.

131. De Nicola A, Hezaveh S, Zhao Y. Micellar drug nanocarriers and biomembranes: how do they interact?. *Physical Chemistry Chemical Physics*. 2014; 16(11): 5093-5105.
132. Mukhija A, Kishore N. Drug partitioning in individual and mixed micelles and interaction with protein upon delivery form micellar media. *Journal of Molecular Liquids*. 2018; 265: 1-15.

Discover a bigger Impact and Visibility of your article publication with Peertechz Publications

Highlights

- ❖ Signatory publisher of ORCID
- ❖ Signatory Publisher of DORA (San Francisco Declaration on Research Assessment)
- ❖ Articles archived in worlds' renowned service providers such as Portico, CNKI, AGRIS, TDNet, Base (Bielefeld University Library), CrossRef, Scilit, J-Gate etc.
- ❖ Journals indexed in ICMJE, SHERPA/ROMEO, Google Scholar etc.
- ❖ OAI-PMH (Open Archives Initiative Protocol for Metadata Harvesting)
- ❖ Dedicated Editorial Board for every journal
- ❖ Accurate and rapid peer-review process
- ❖ Increased citations of published articles through promotions
- ❖ Reduced timeline for article publication

Submit your articles and experience a new surge in publication services
(<https://www.peertechz.com/submission>).

Peertechz journals wishes everlasting success in your every endeavours.